

Evidence for Multimodal Superfluidity in Neutrons and Other Emergent Phenomena & Parametric Matrix Models

Dean Lee
Facility for Rare Isotope Beams
Michigan State University
Nuclear Lattice EFT Collaboration

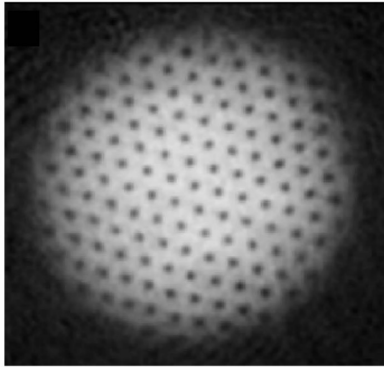
Next Generation Ab Initio Nuclear Theory
ECT*, Trento
July 17, 2025



Part I: Evidence for Multimodal Superfluidity in Neutrons
and Other Emergent Phenomena

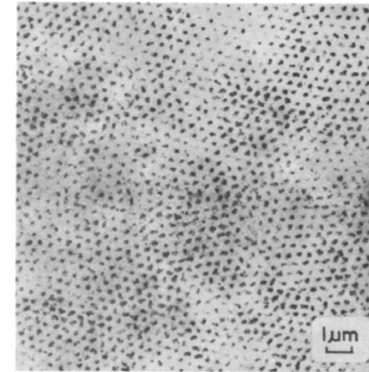
Superfluid condensation

BEC Theory



Ketterle, Zwierlein,
Ultracold Fermi Gases (2008)

BCS Theory



Essmann, Träuble,
Physics Letters A 27, 3 (1968)



Off-diagonal long-range order

Bosonic superfluidity

$$\langle \Psi_0 | a^\dagger(\mathbf{r}) a(\mathbf{0}) | \Psi_0 \rangle$$

Fermionic superfluidity (S-wave)

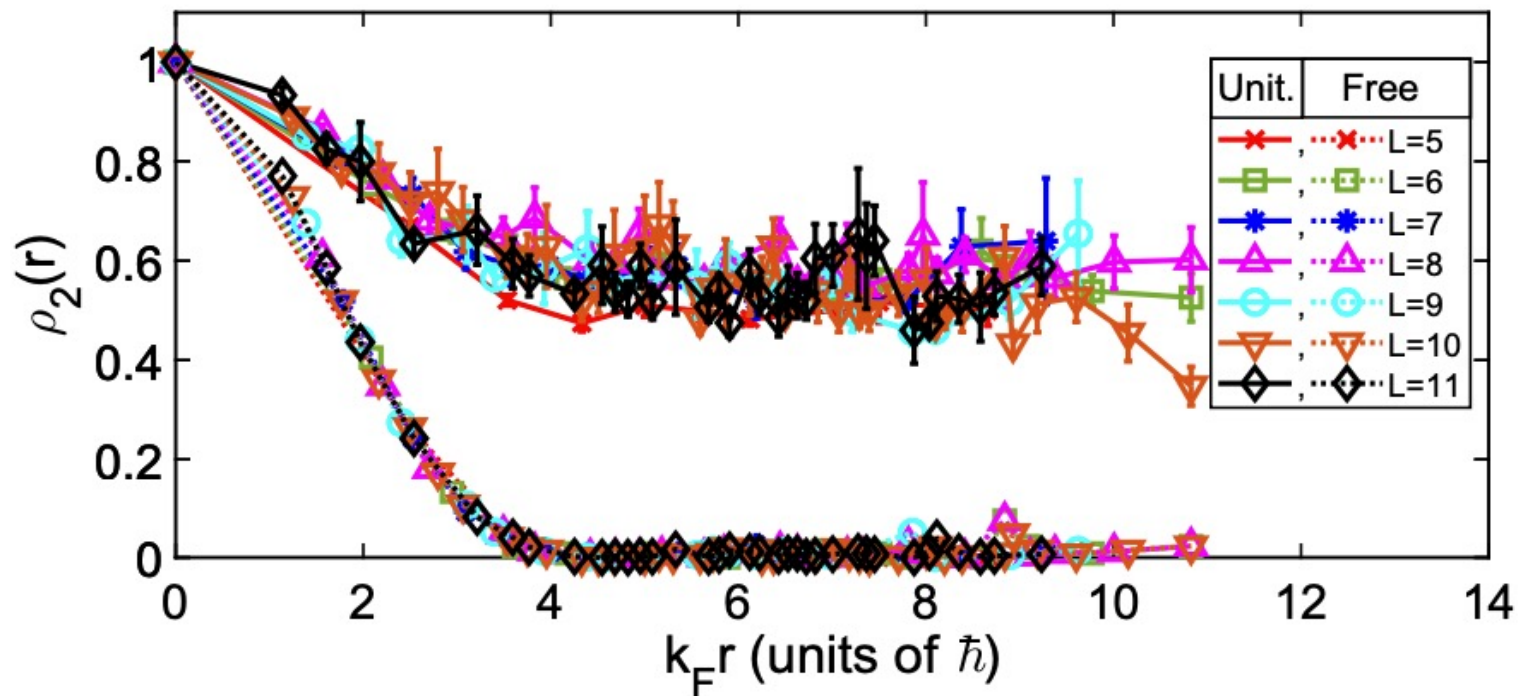
$$\langle \Psi_0 | a_\downarrow^\dagger(\mathbf{r}) a_\uparrow^\dagger(\mathbf{r}) a_\uparrow(\mathbf{0}) a_\downarrow(\mathbf{0}) | \Psi_0 \rangle$$

Fermionic superfluidity (P-wave)

$$\langle \Psi_0 | a_\uparrow^\dagger(\mathbf{r}) a_\uparrow^\dagger(\mathbf{r} + \Delta\mathbf{r}) a_\uparrow(\Delta\mathbf{r}) a_\uparrow(\mathbf{0}) | \Psi_0 \rangle$$

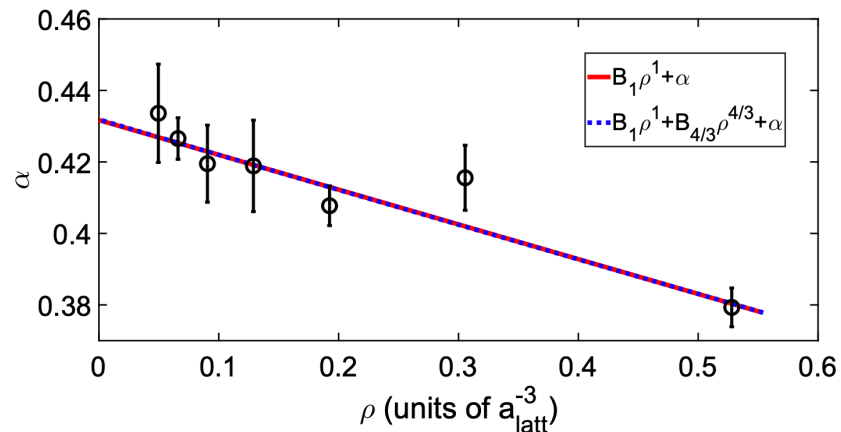
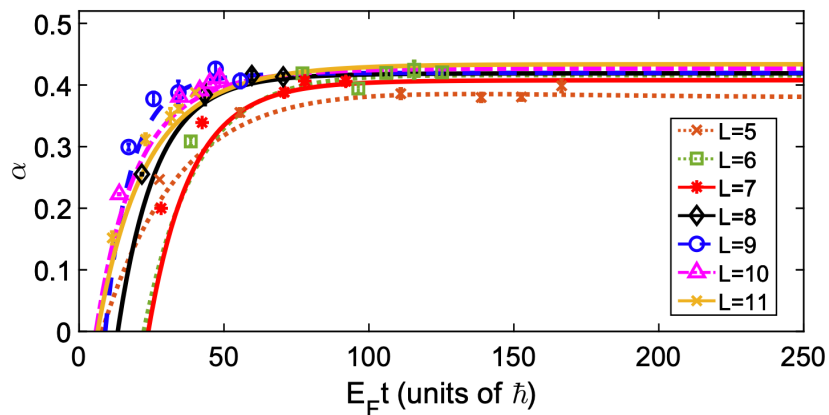
Yang, RMP **34**, 694 (1962)

Unitary limit



He, Li, Lu, D.L., Phys. Rev. A 101, 063615 (2020)

Unitary limit



condensate fraction = 0.43(2)

He, Li, Lu, D.L., Phys. Rev. A 101, 063615 (2020)

${}^6\text{Li}$ experiments: 0.46(7) [1, 2] and 0.47(7) [3]

[1] Zwierlein, Stan, Schunck, Raupach, Kerman, Ketterle, PRL 92, 120403 (2004).

[2] Zwierlein, Schunck, Stan, Raupach, Ketterle, PRL 94, 180401 (2005).

[3] Kwon, Pace, Panza, Inguscio, Zwirger, Zaccanti, Scazza, Roati, Science 369, 84 (2020).

Attractive extended Hubbard models

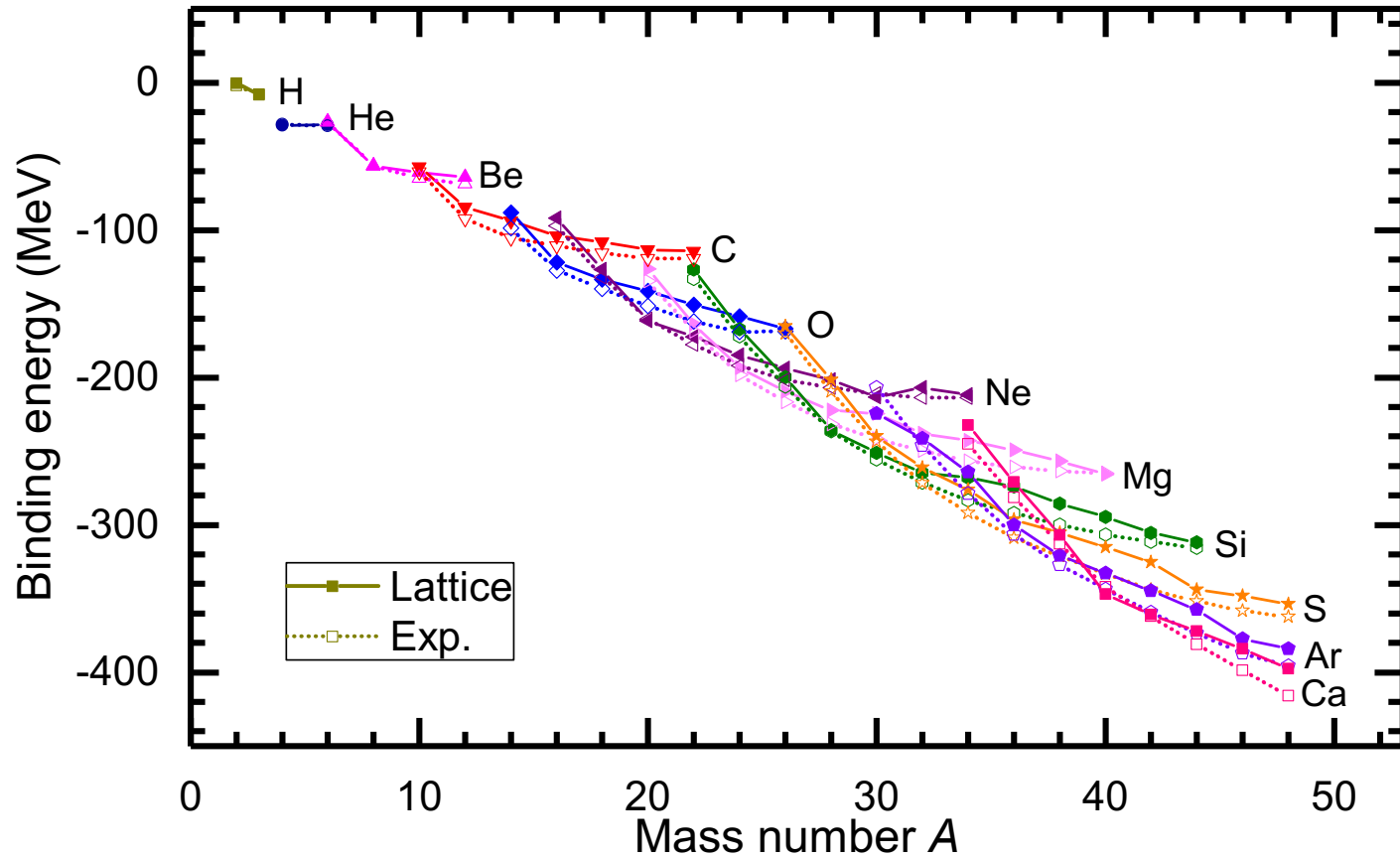
We consider attractive extended Hubbard models for two-component fermions in 1, 2, 3 dimensions

$$H = H_{\text{free}} + \frac{1}{2}C_2 \sum_{\mathbf{n}} \tilde{\rho}(\mathbf{n})^2$$

$$\tilde{\rho}(\mathbf{n}) = \sum_{j=\uparrow,\downarrow} \tilde{a}_j^\dagger(\mathbf{n})\tilde{a}_j(\mathbf{n}) + s_L \sum_{|\mathbf{n}-\mathbf{n}'|=1} \sum_{j=\uparrow,\downarrow} \tilde{a}_j^\dagger(\mathbf{n}')\tilde{a}_j(\mathbf{n}')$$

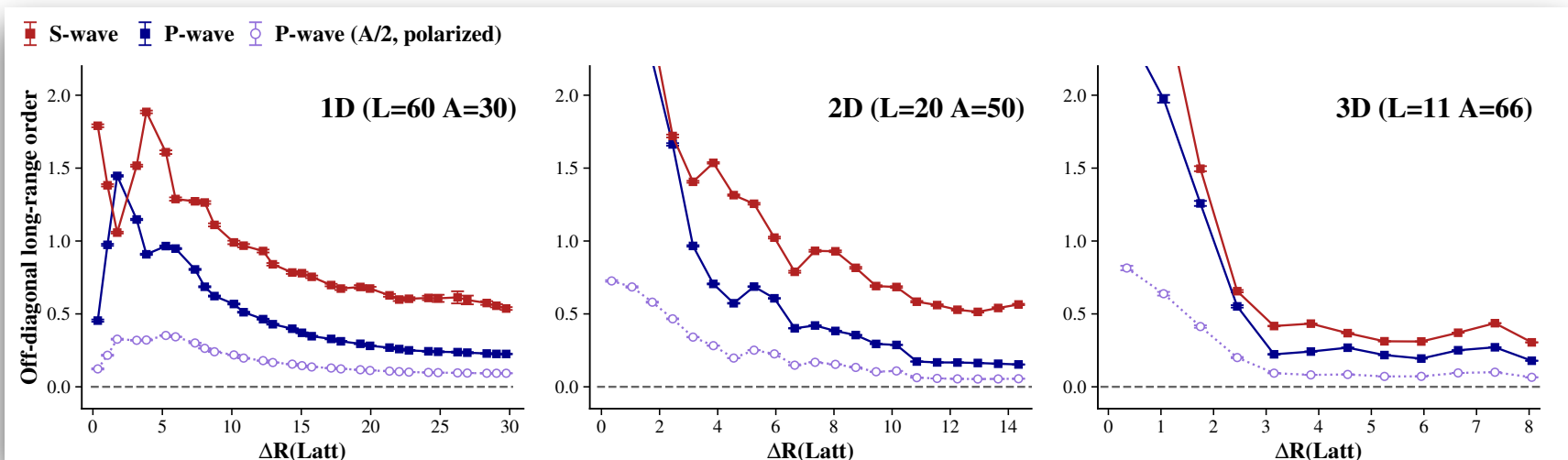
$$\tilde{a}_j(\mathbf{n}) = a_j(\mathbf{n}) + s_{NL} \sum_{|\mathbf{n}-\mathbf{n}'|=1} a_j(\mathbf{n}')$$

While just a toy model, attractive extended Hubbard models are quite useful for nuclear physics. If we include protons, a three-body interaction, and Coulomb interactions, we can reproduce the binding energies of light and medium-mass nuclei fairly well.



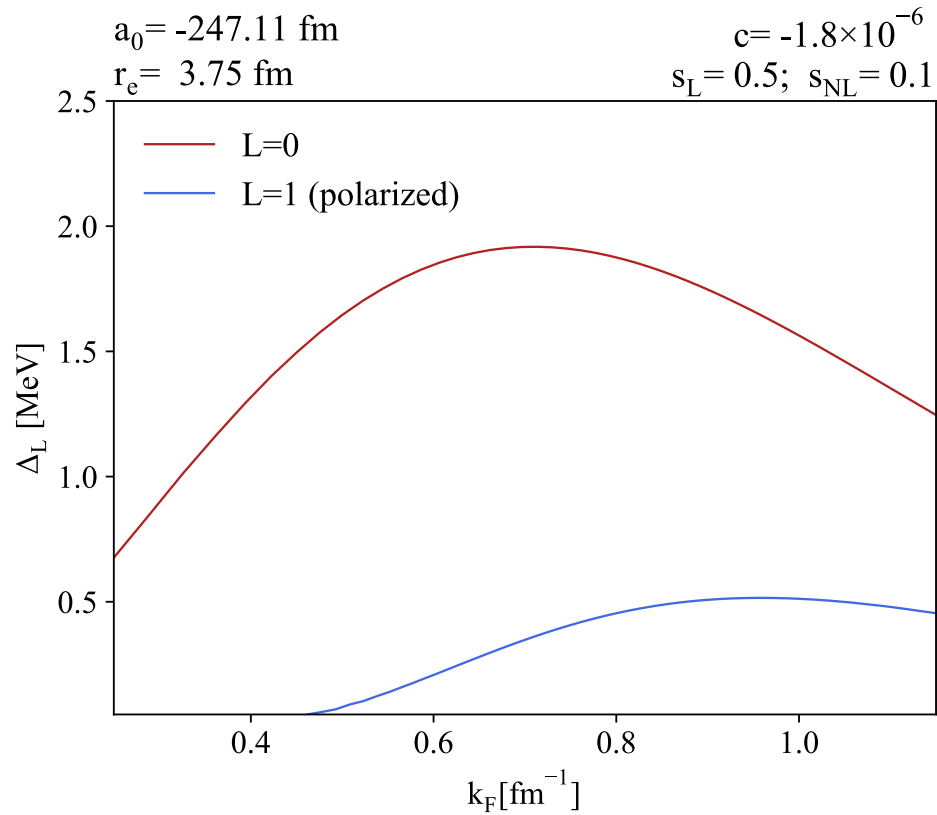
Lu, Li, Elhatisari, D.L., Epelbaum, Meißner, Phys. Lett. B 797, 134863 (2019)

But our focus here is on pure neutron systems. The 1D system is a Luttinger liquid. The 1D condensate fraction decreases as a negative fractional power of the number of particles.

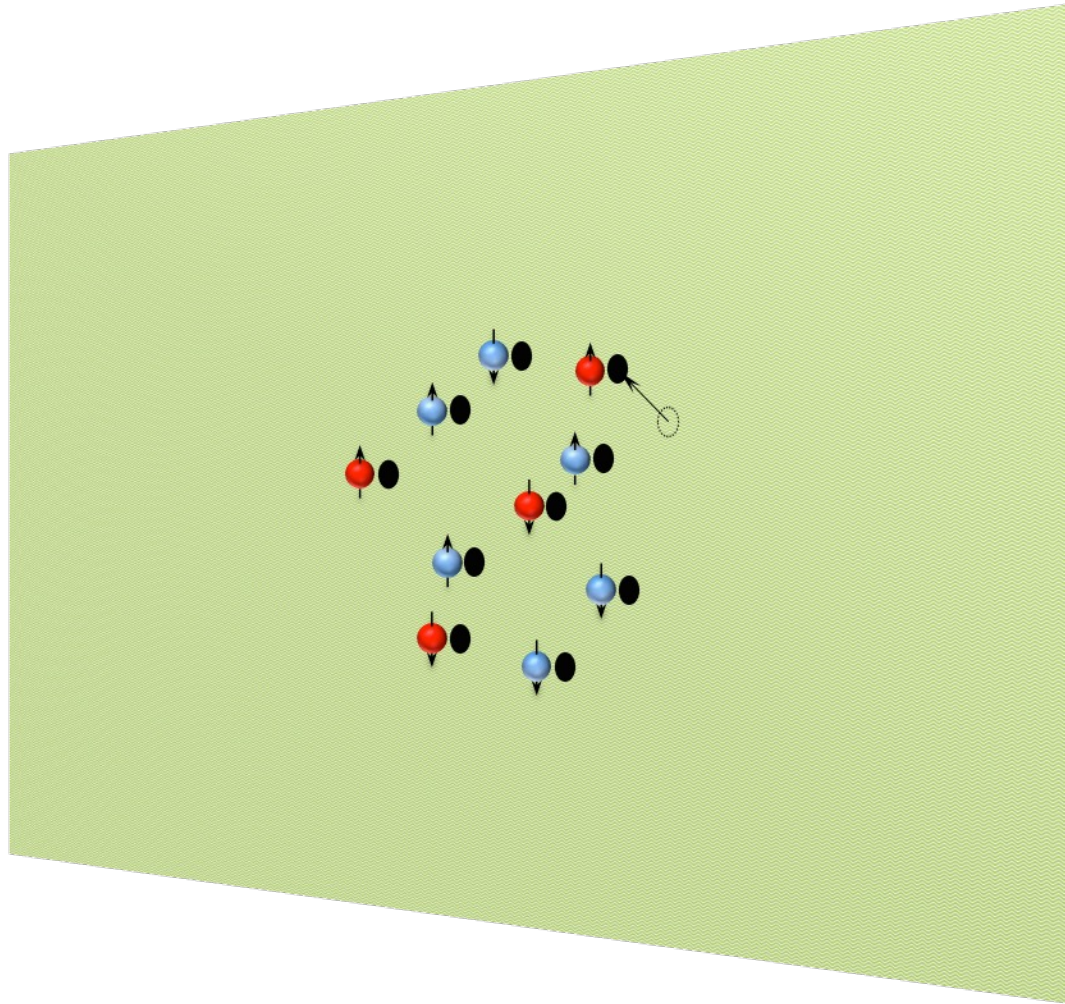


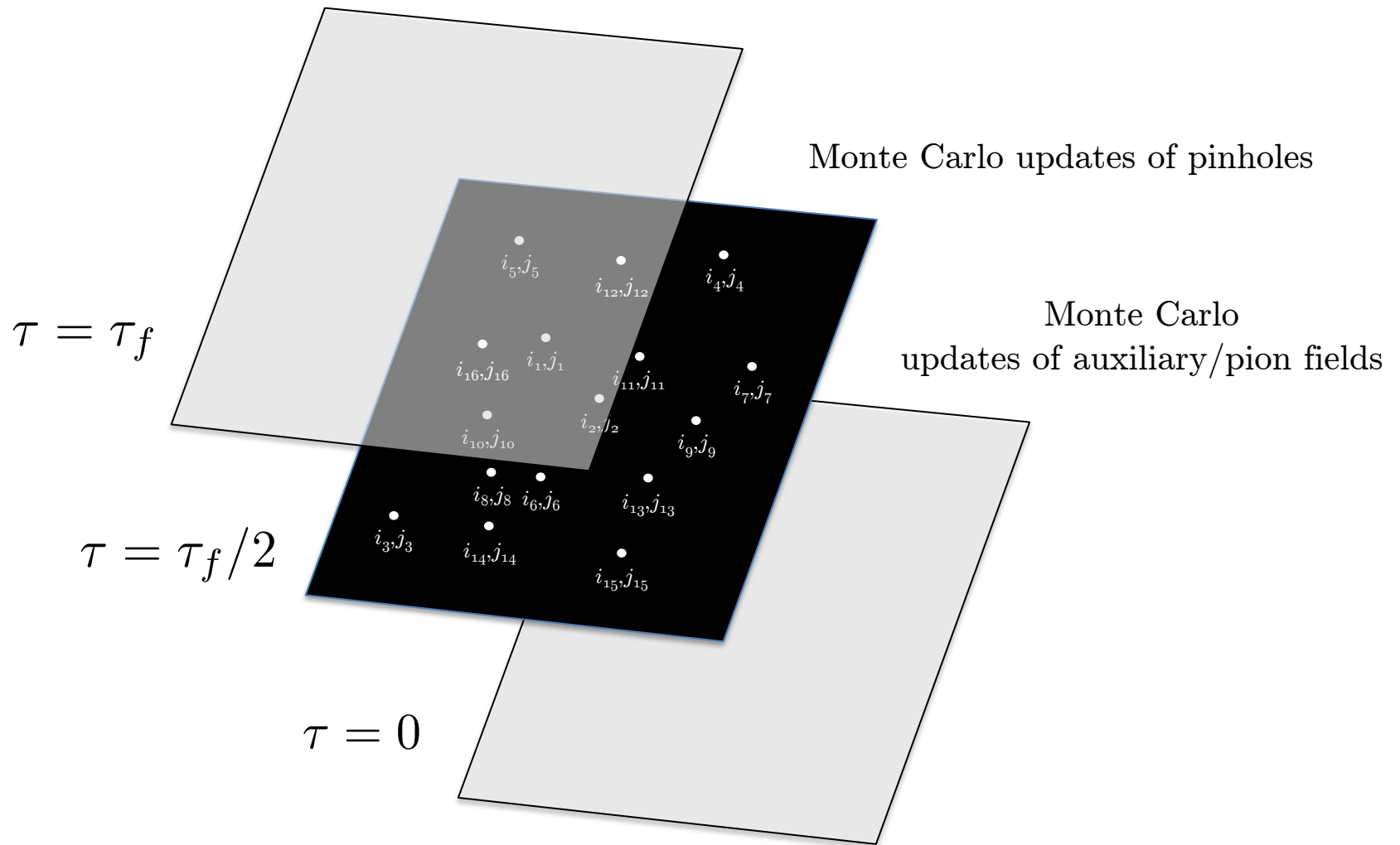
Ma, Palkanoglou, Carlson, Gandolfi, Gezerlis, D.L., Schmidt, Yu, in progress

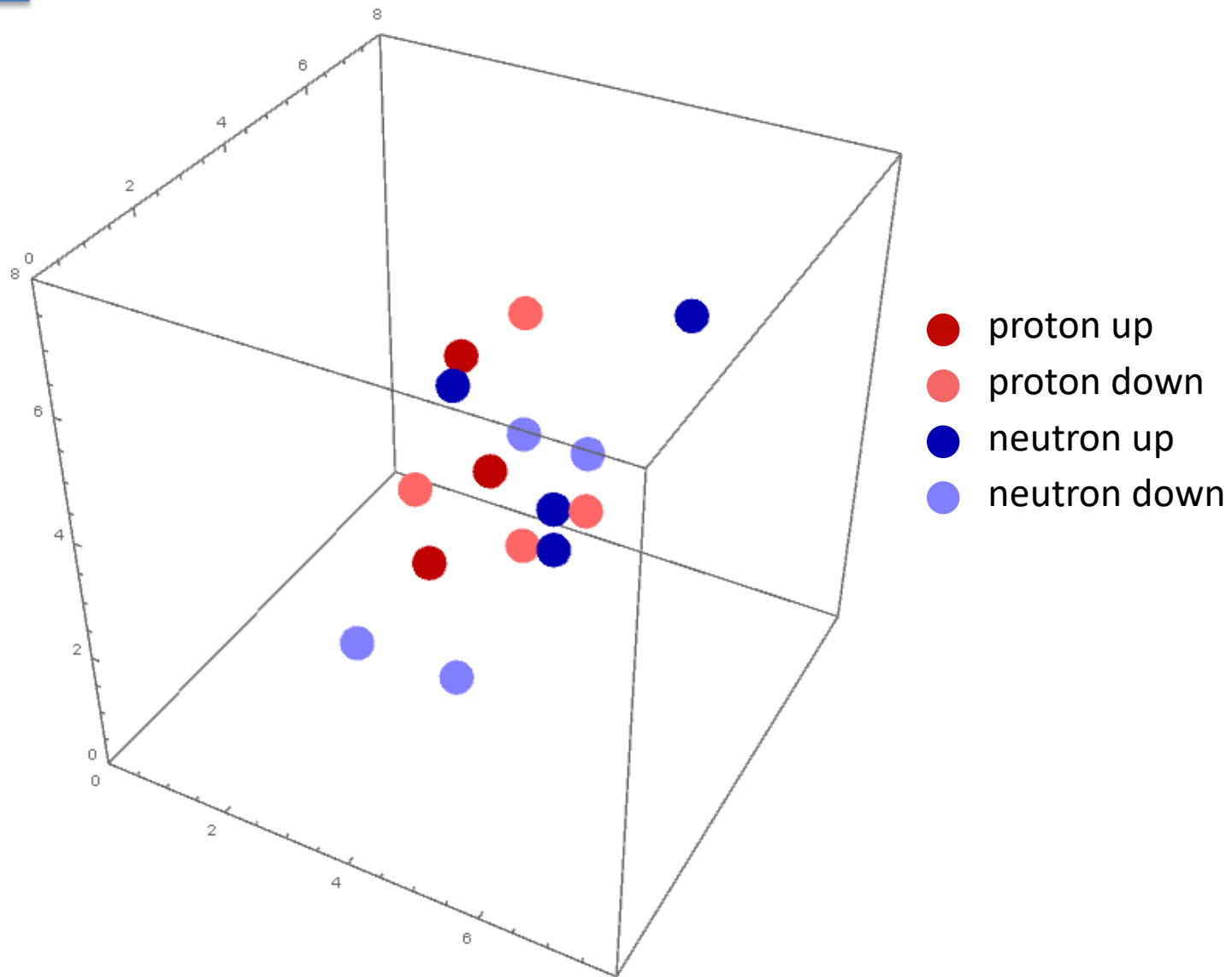
BCS results in three dimensions

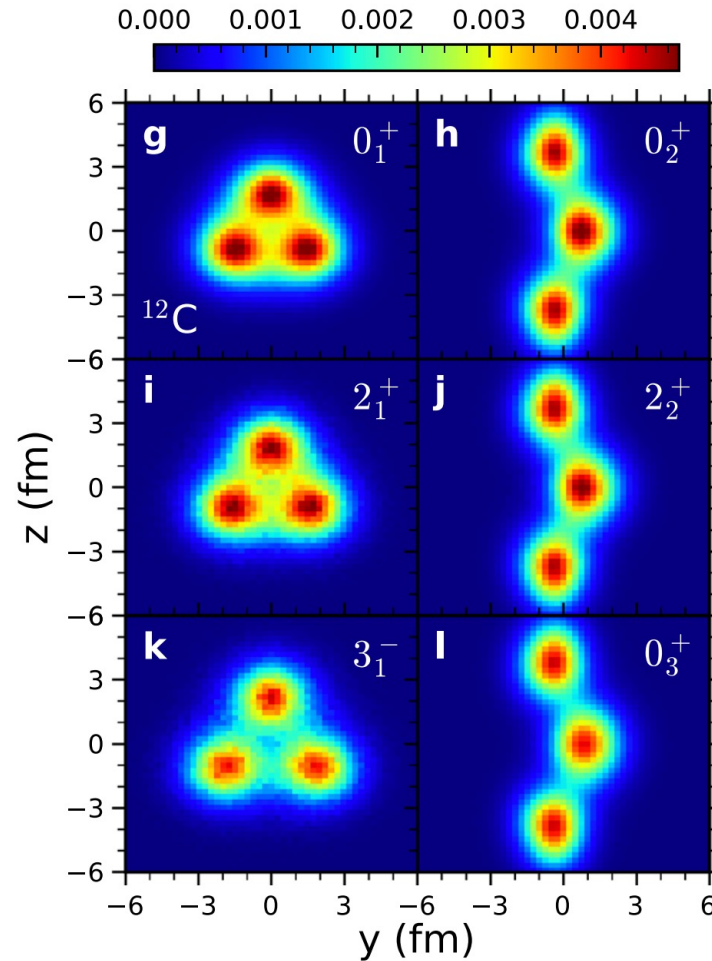


Pinhole algorithm

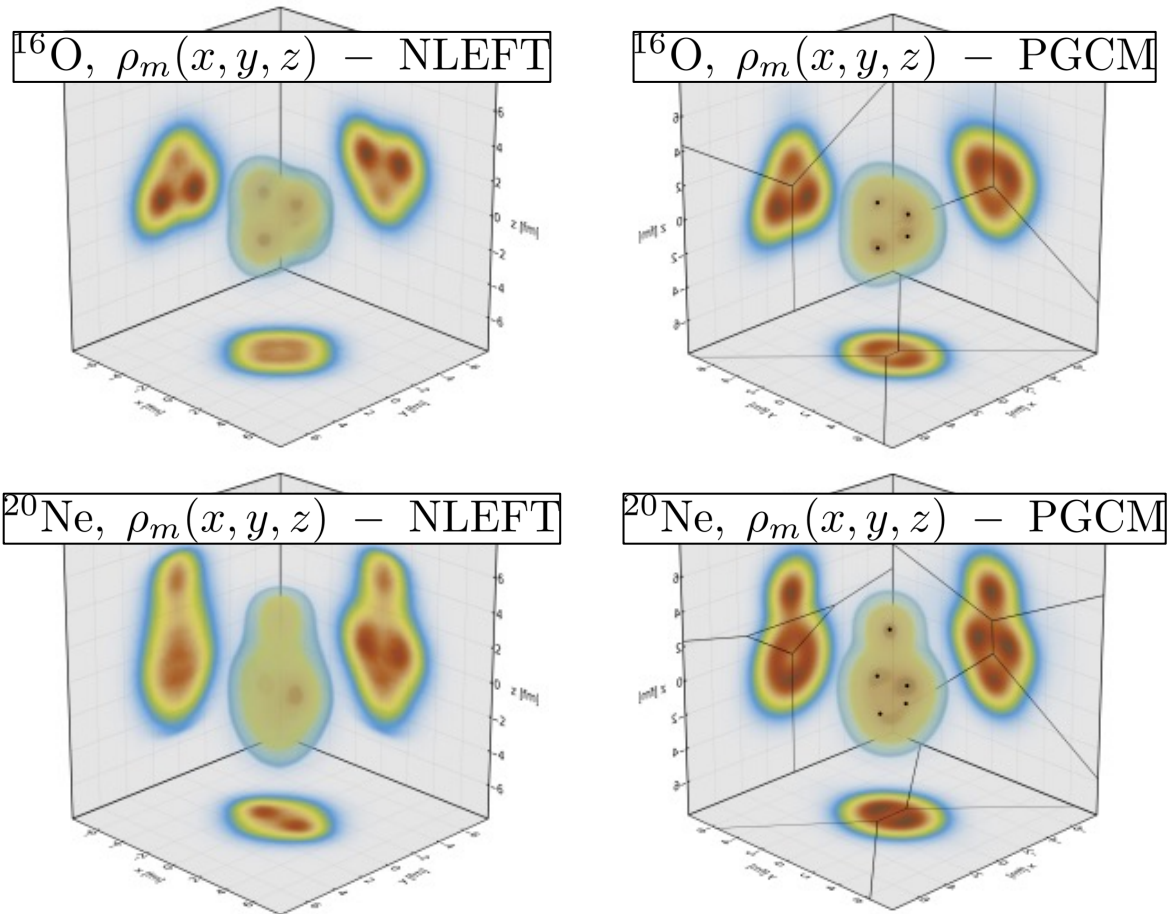




^{16}O 

Structure of ^{12}C 

Shen, Elhatisari, Lähde, D.L., Lu, Meißner, Nat. Commun. 14, 2777 (2023)

Structure of ^{16}O and ^{20}Ne 

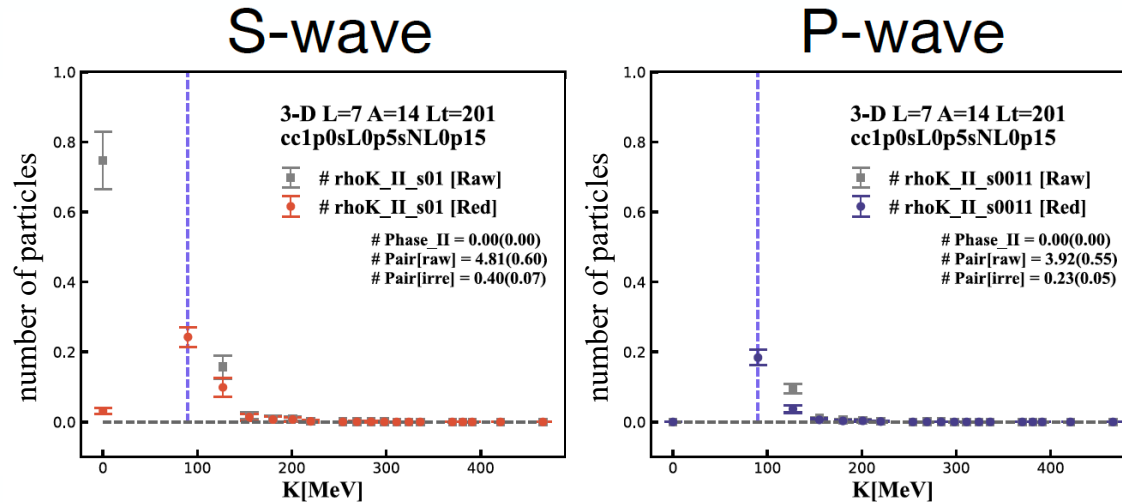
Giacalone et al., arXiv:2402.05995, Phys. Rev. Lett. in press

Giacalone et al., Phys. Rev. Lett. 134, 082301 (2025)

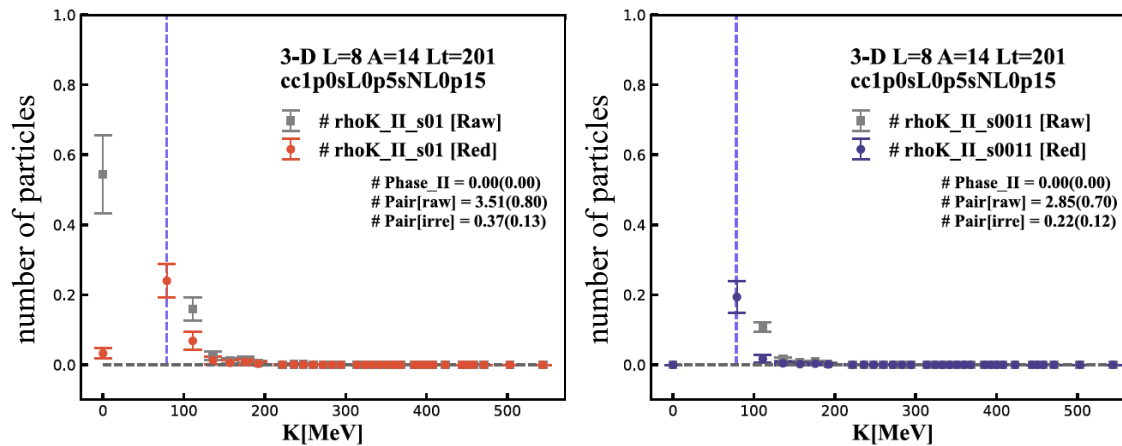
3D attractive extended Hubbard model

Momentum-space pinhole algorithm

L=7



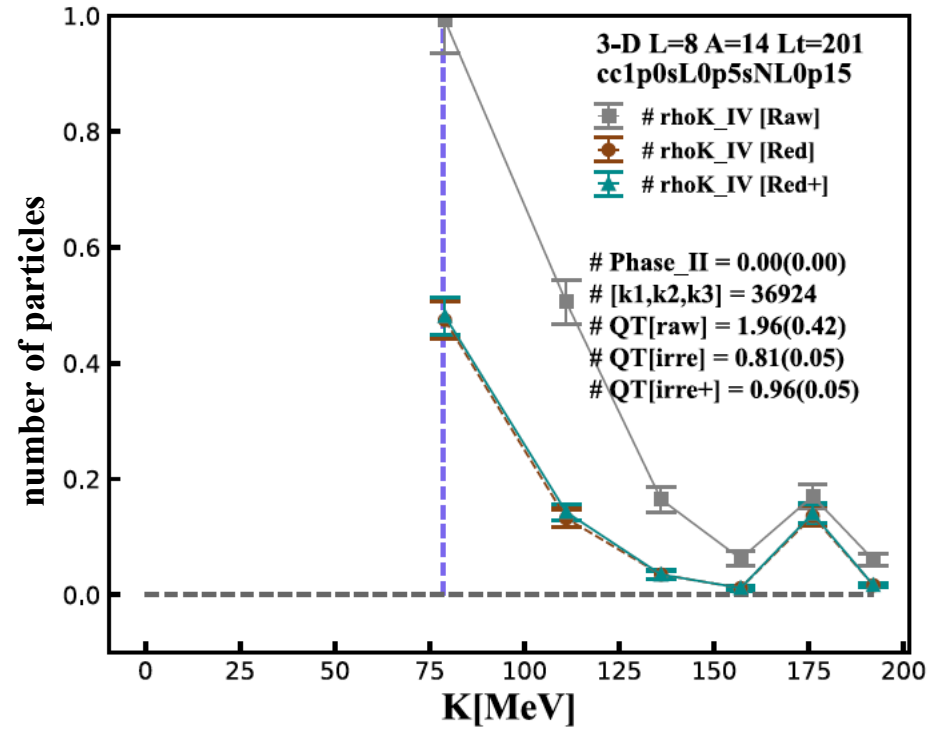
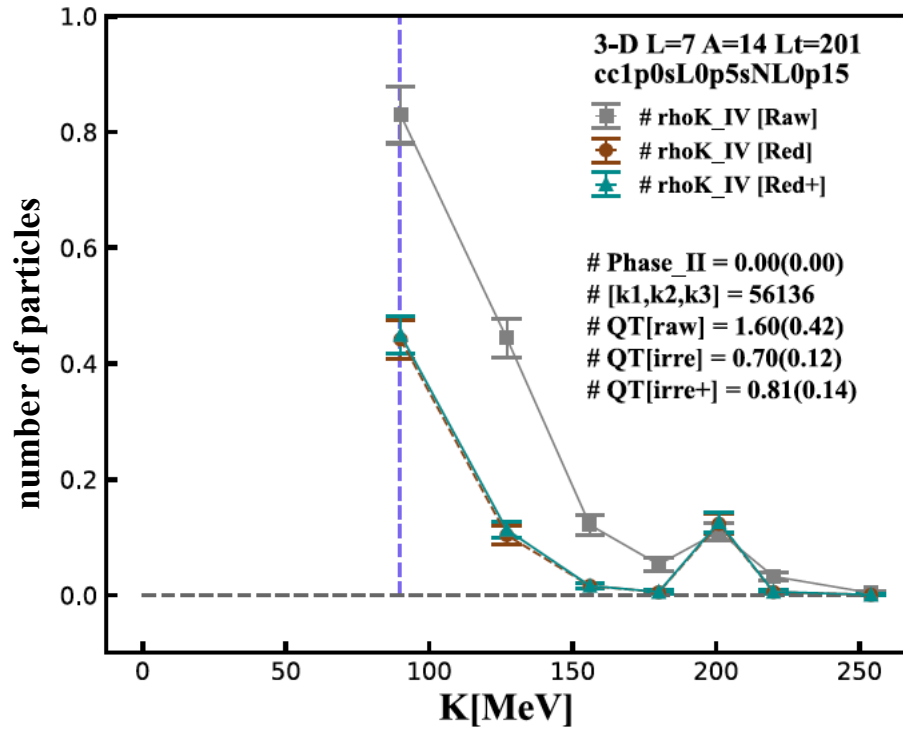
L=8



Ma, Palkanoglou, Carlson, Gandolfi, Gezerlis, D.L., Schmidt, Yu, in progress

Multimodal superfluidity

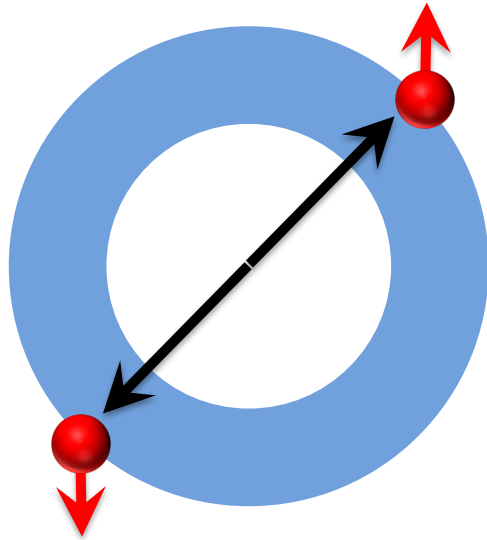
An unexpected guest: quartets



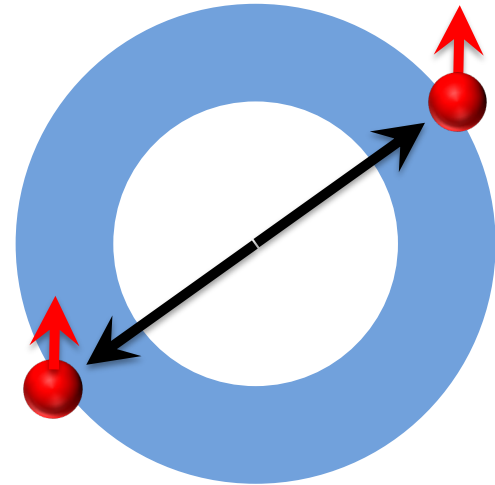
Ma, Palkanoglou, Carlson, Gandolfi, Gezerlis, D.L., Schmidt, Yu, in progress

Multimodal superfluidity

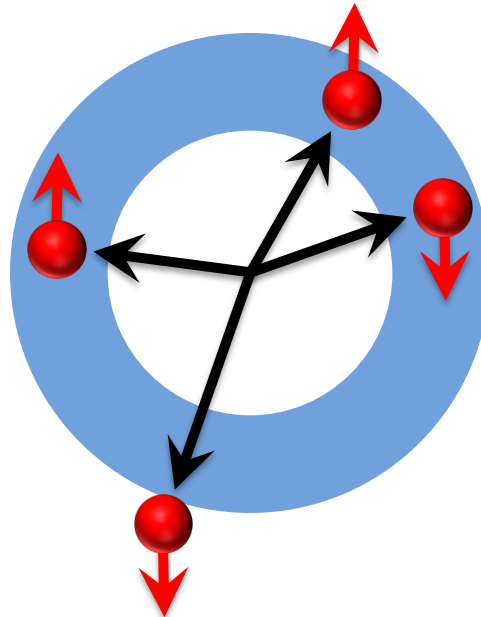
singlet pair



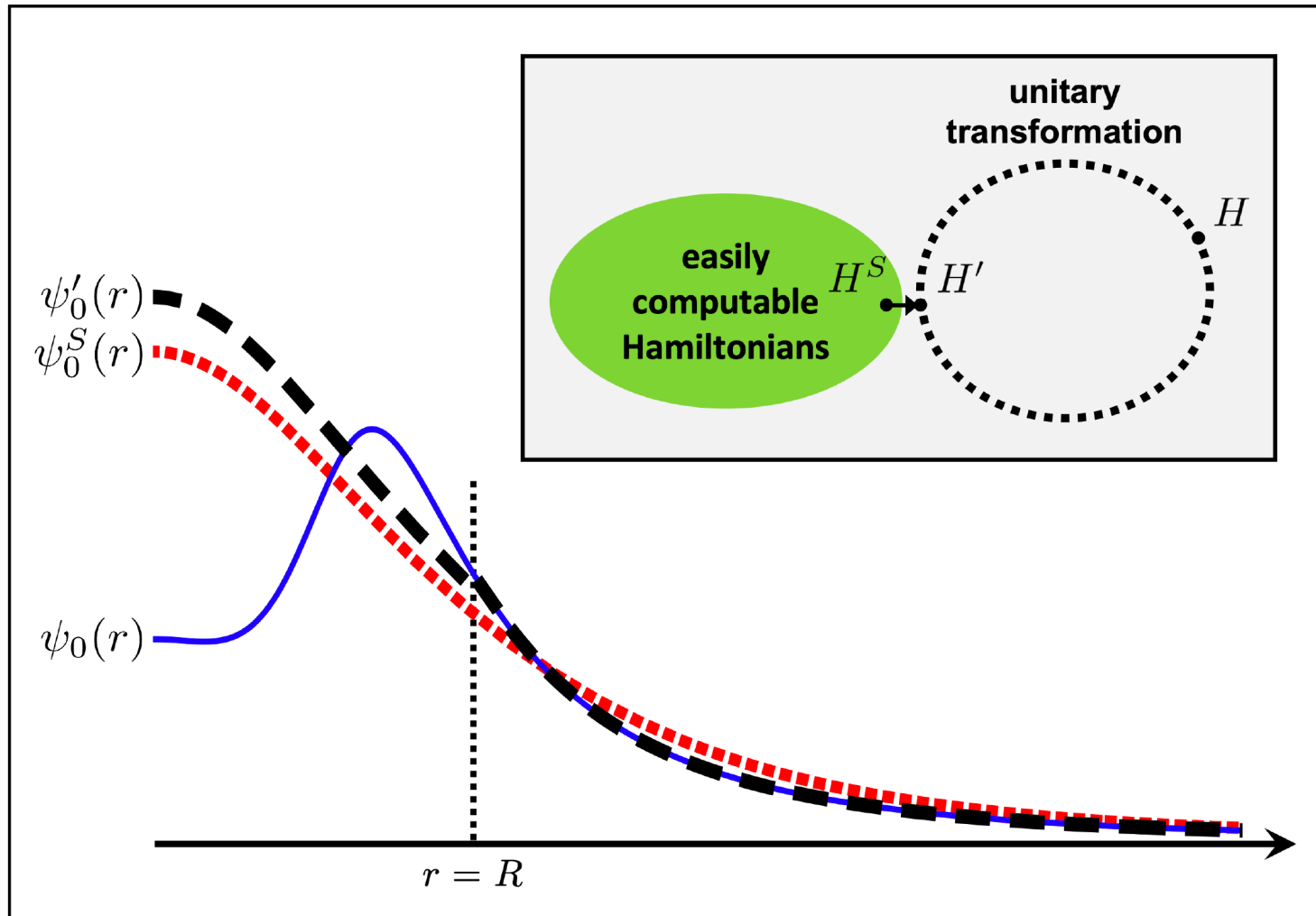
triplet pair



quartet

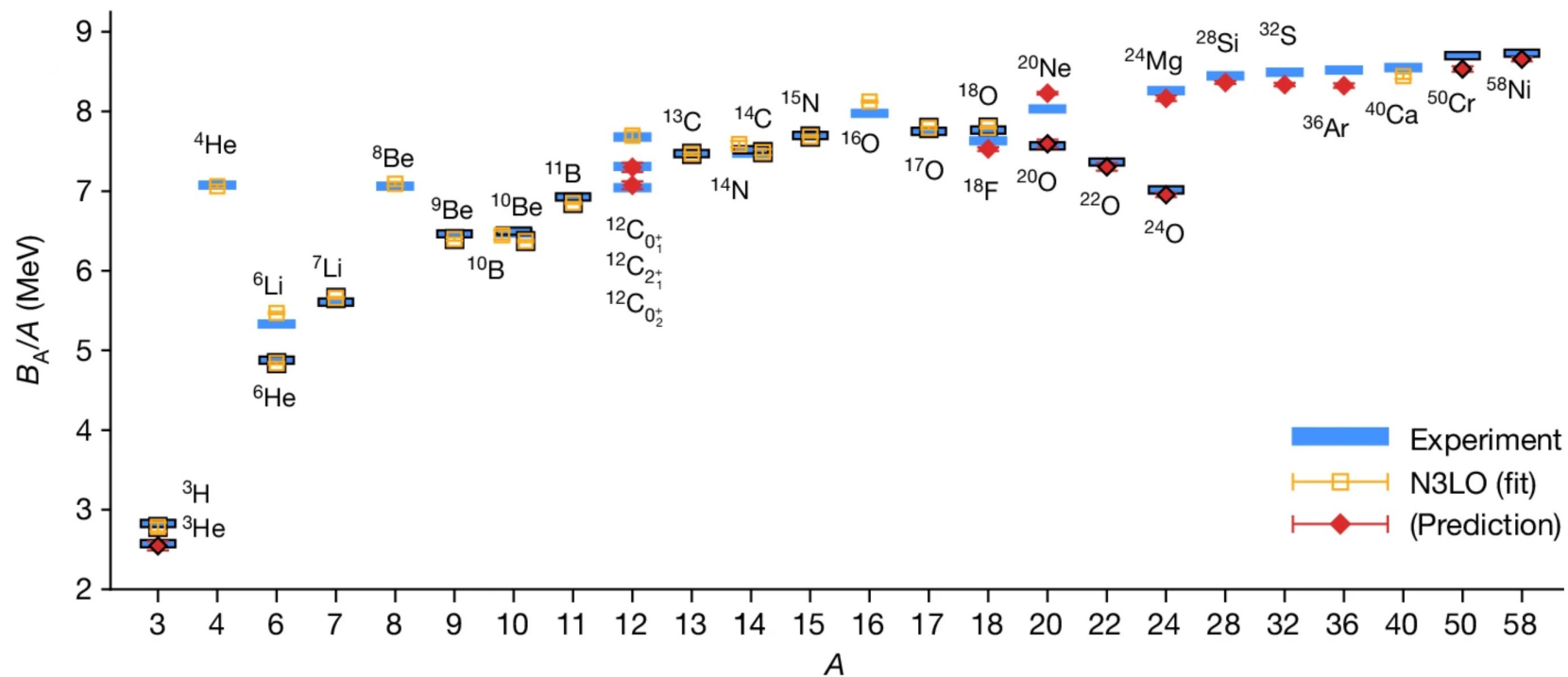


Wavefunction matching



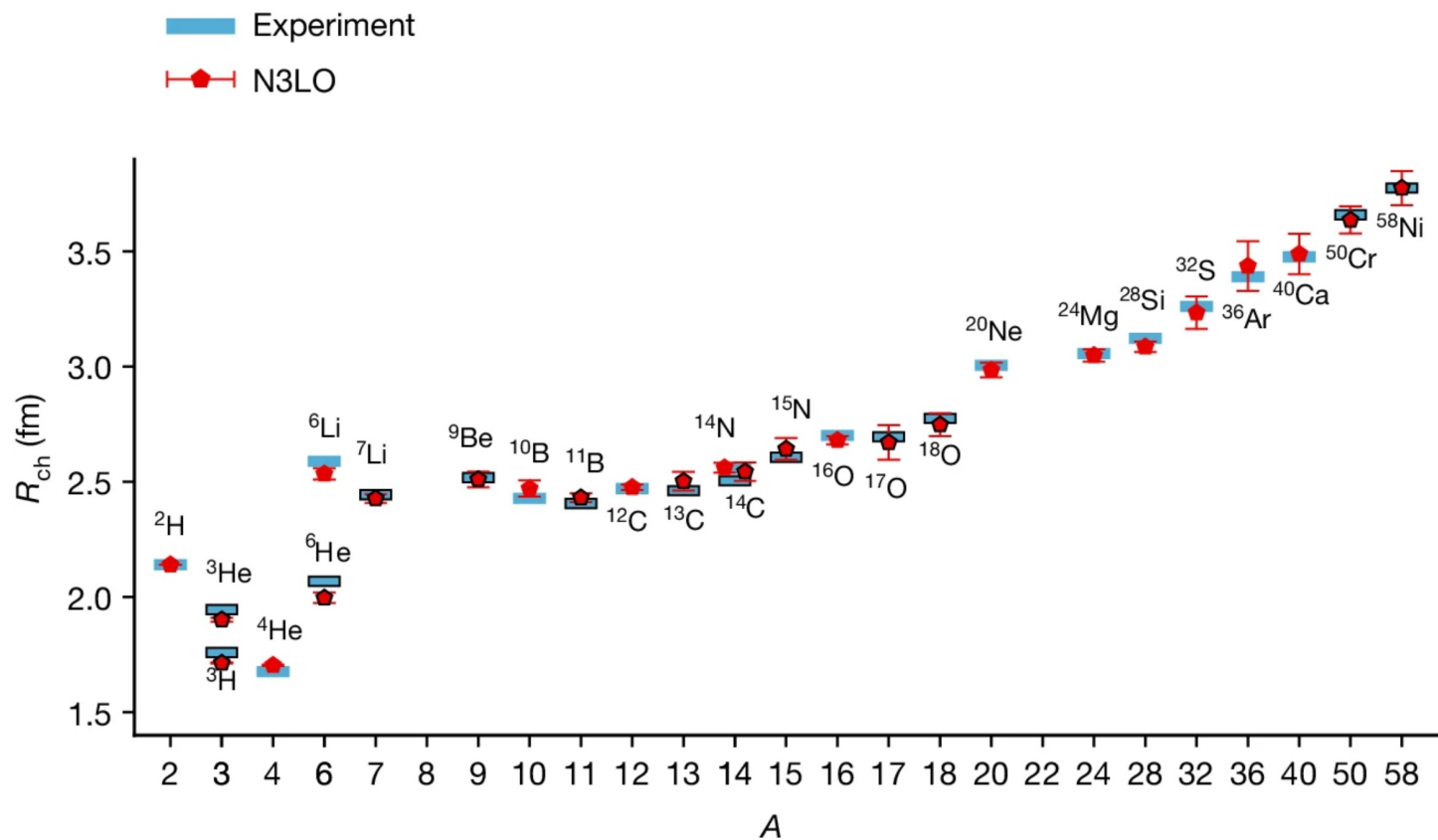
Elhatisari, Bovermann, Ma, Epelbaum, Frame, Hildenbrand, Krebs, Lähde, D.L., Li, Lu, M. Kim, Y. Kim, Meißner, Rupak, Shen, Song, Stellin, Nature 630, 59 (2024)

Binding energies



Elhatisari, Bovermann, Ma, Epelbaum, Frame, Hildenbrand, Krebs, Lähde, D.L., Li, Lu, M. Kim, Y. Kim, Meißner, Rupak, Shen, Song, Stellin, Nature 630, 59 (2024)

Charge radii



Elhatisari, Bovermann, Ma, Epelbaum, Frame, Hildenbrand, Krebs, Lähde, D.L., Li, Lu, M. Kim, Y. Kim, Meißner, Rupak, Shen, Song, Stellin, Nature 630, 59 (2024)

Neutron and nuclear matter

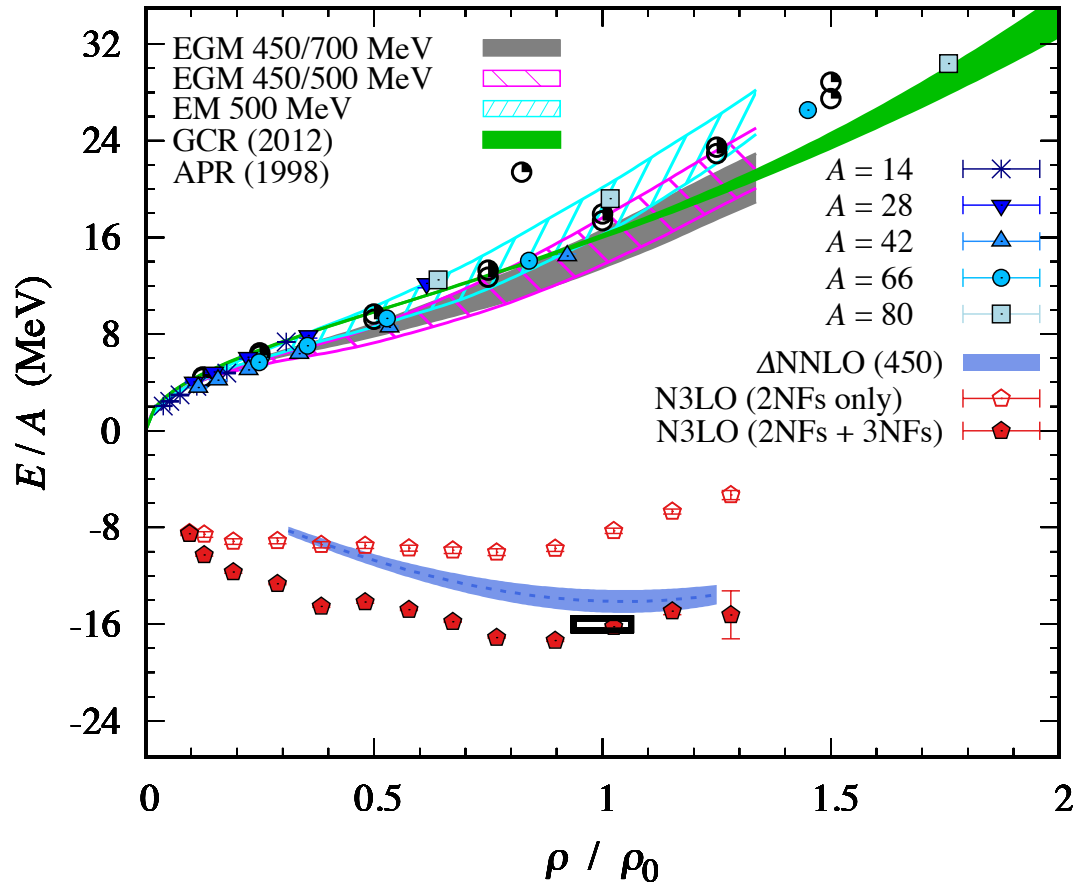
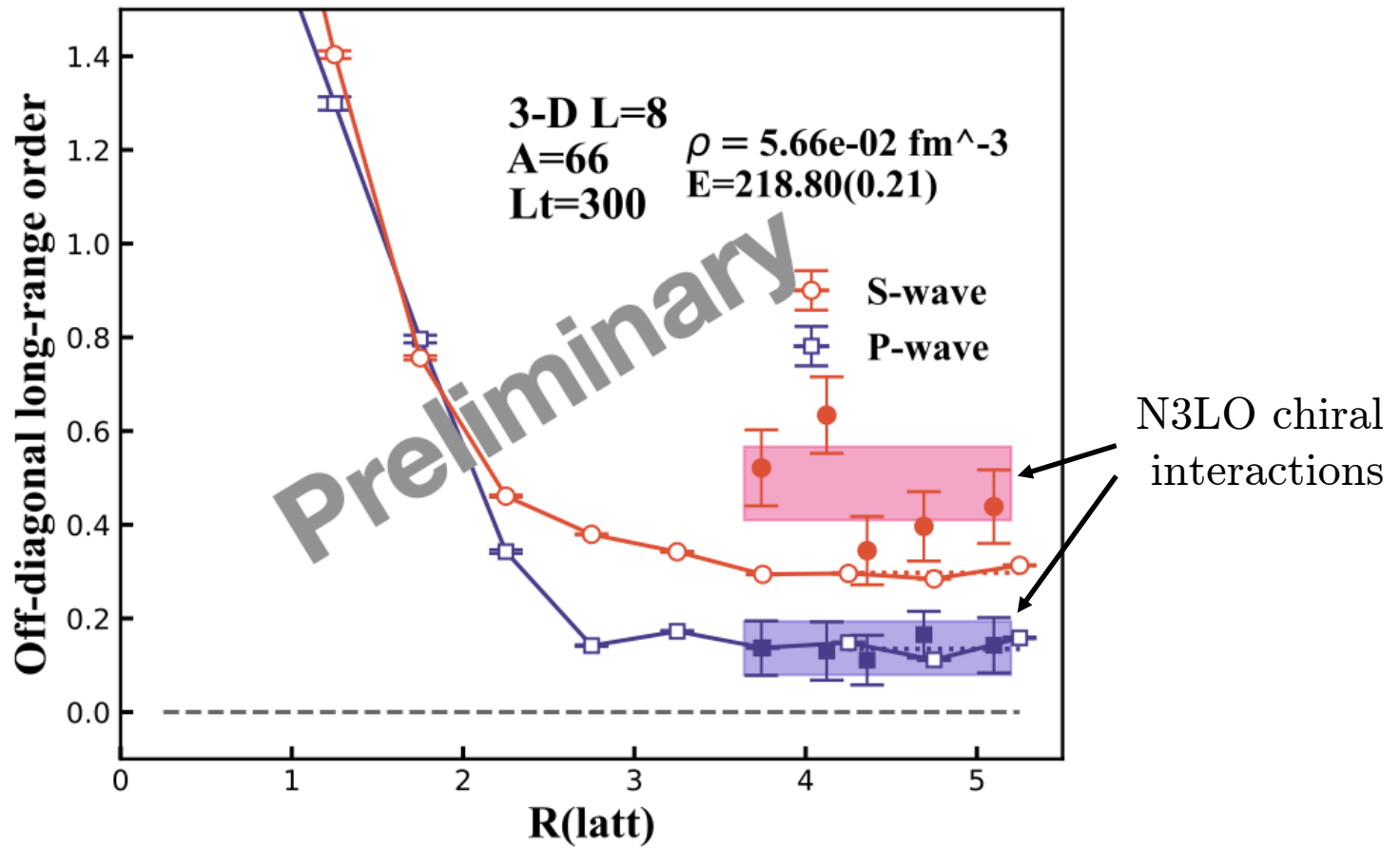


Figure adapted from Tews, Krüger, Hebeler, Schwenk, Phys. Rev. Lett. 110, 032504 (2013)

Elhatisari, Bovermann, Ma, Epelbaum, Frame, Hildenbrand, Krebs, Lähde, D.L., Li, Lu, M. Kim, Y. Kim, Meißner, Rupak, Shen, Song, Stellin, Nature 630, 59 (2024)

Multimodal superfluidity of neutrons



Ma, Palkanoglou, Carlson, Gandolfi, Gezerlis, D.L., Schmidt, Yu, in progress

Multimodal superfluidity of neutrons

$$N_{\uparrow} = 19, N_{\downarrow} = 19$$

$$N_{\uparrow} = 20, N_{\downarrow} = 19$$

$$N_{\uparrow} = 21, N_{\downarrow} = 19$$

$$N_{\uparrow} = 20, N_{\downarrow} = 20$$

$$L^3 = (9.21 \text{ fm})^3$$

$$k_F = 190 \text{ MeV}$$

$$E_F = 19 \text{ MeV}$$

$$\Delta_{1S_0} = 3.4(6) \text{ MeV}$$

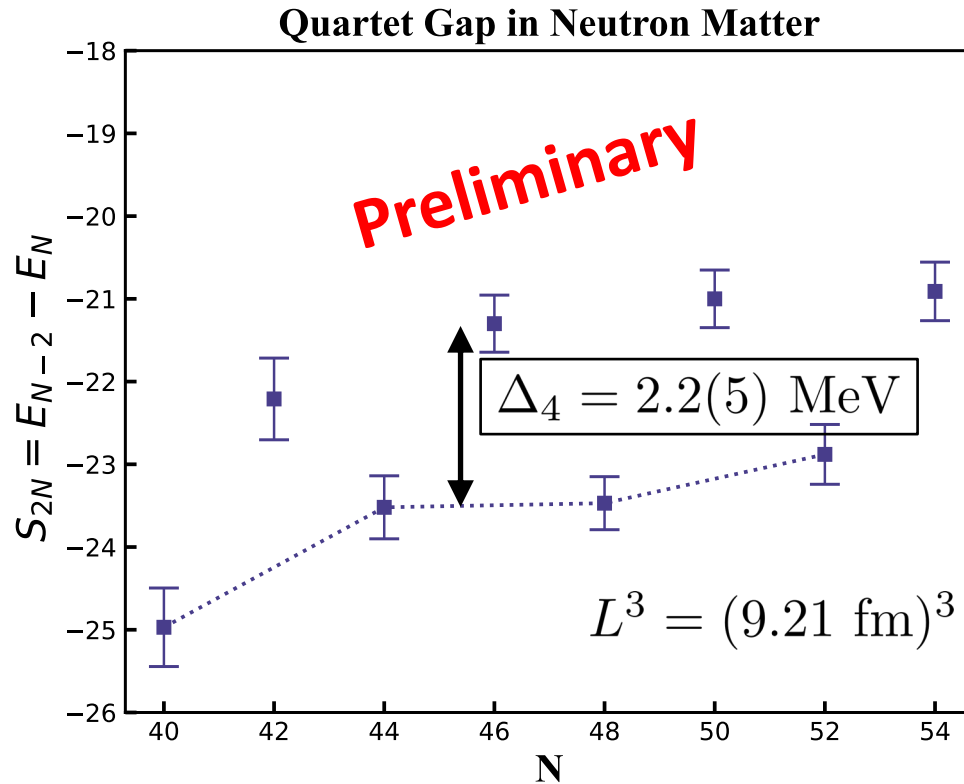
$$\Delta_{3P_0} = 1.0(5) \text{ MeV}$$

$$\Delta_{3P_1} = -0.1(7) \text{ MeV}$$

$$\Delta_{3P_2} = 1.1(6) \text{ MeV}$$

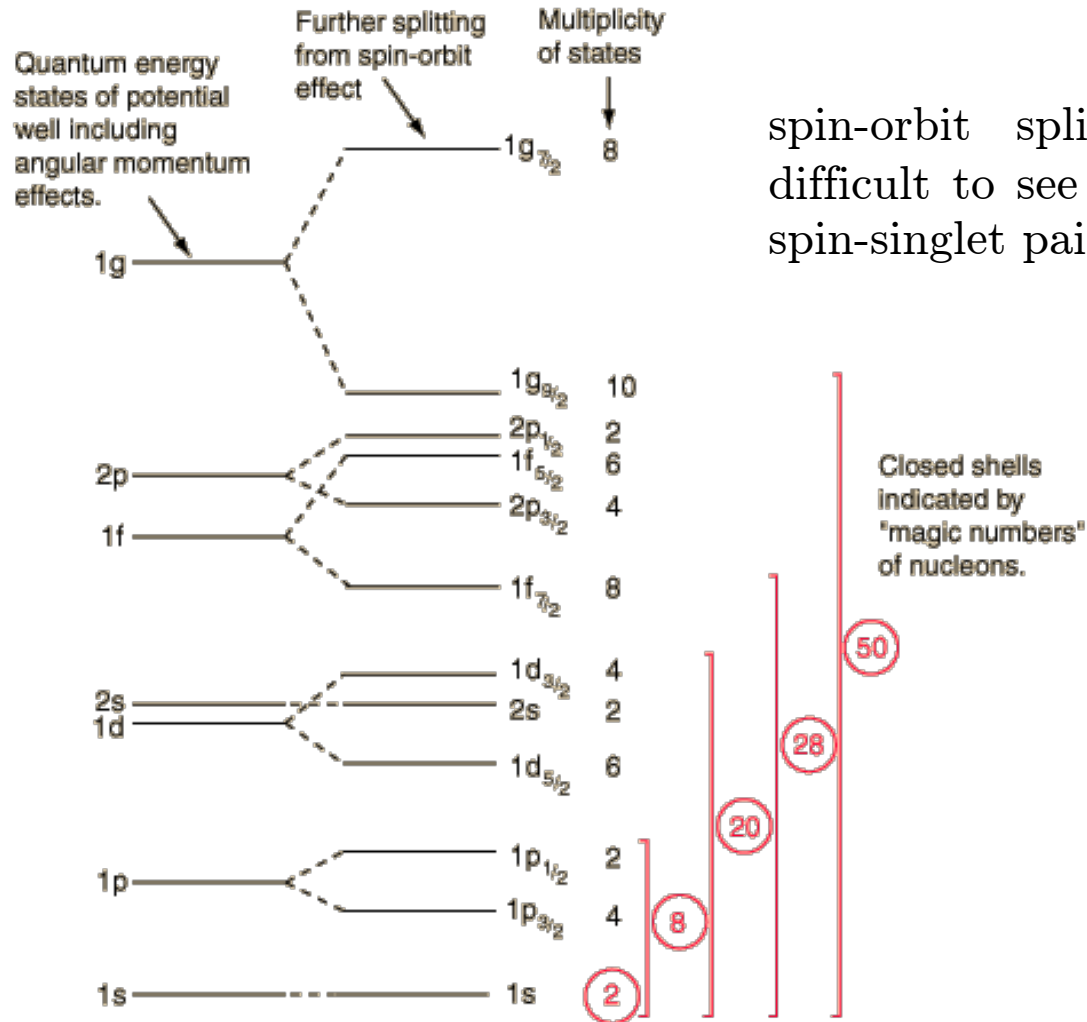
Preliminary

Multimodal superfluidity of neutrons



Ma, Palkanoglou, Carlson, Gandolfi, Gezerlis, D.L., Schmidt, Yu, in progress

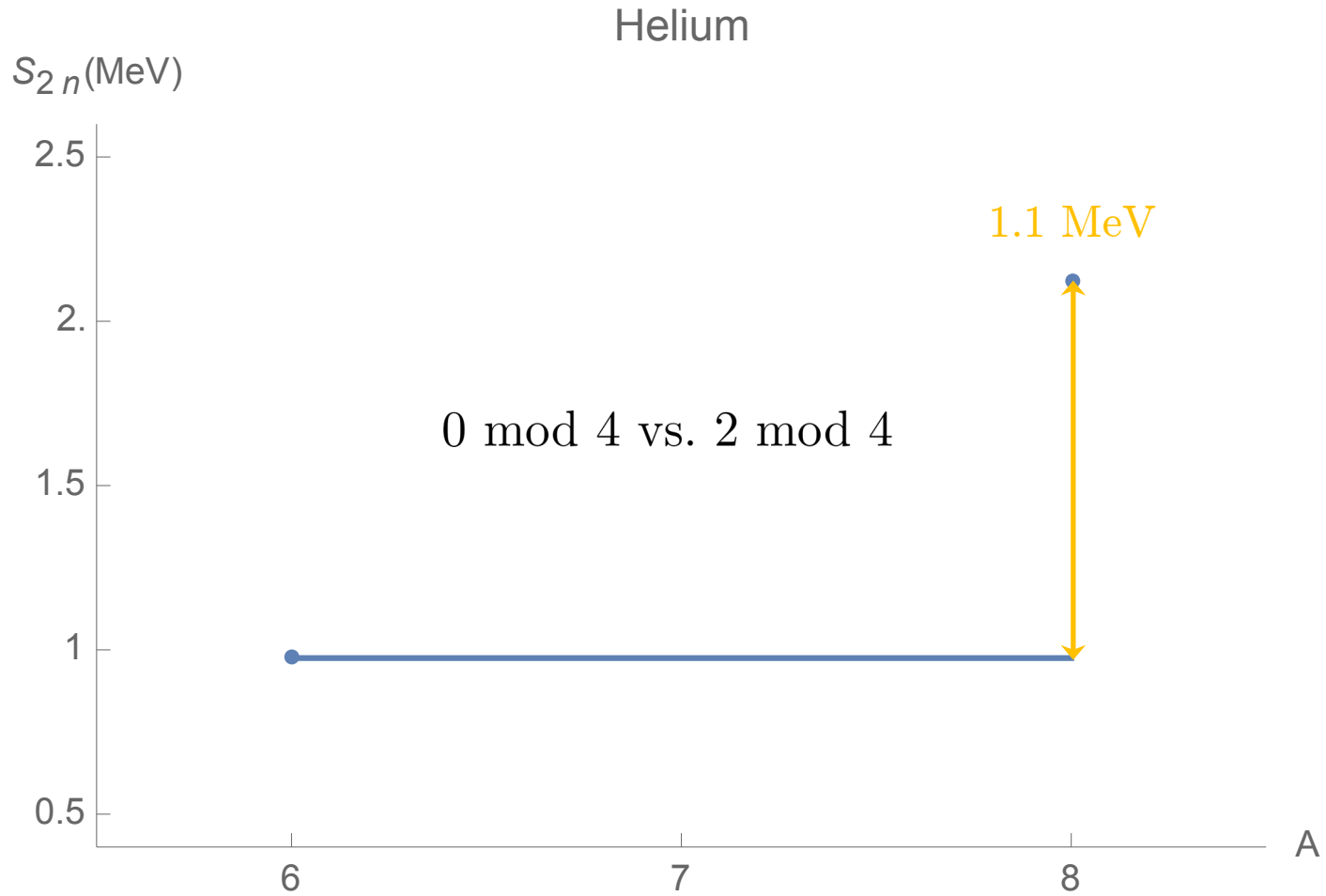
Superfluid condensates in nuclei



spin-orbit splitting makes it difficult to see anything except spin-singlet pairing

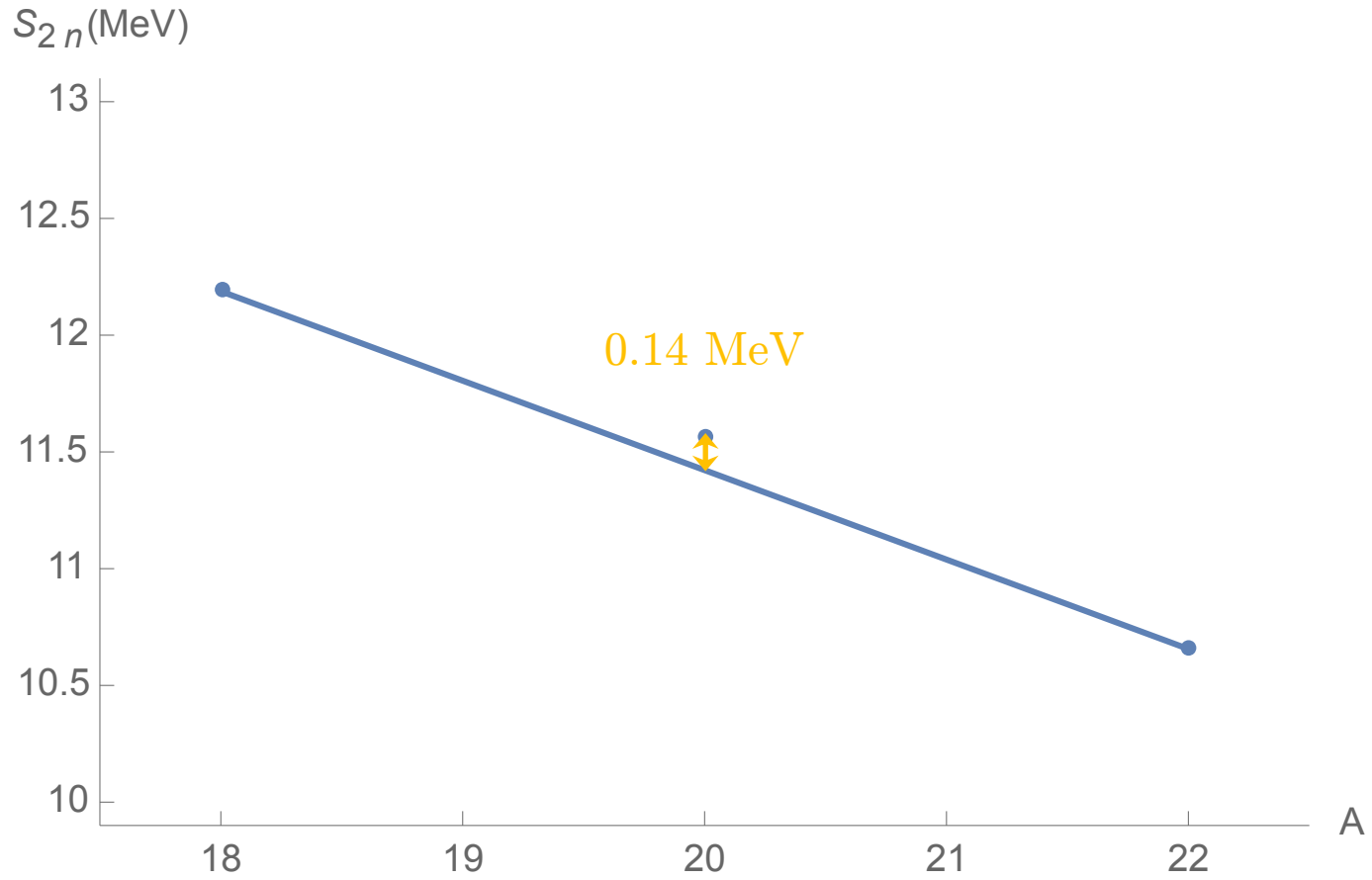
Rohlf, Modern Physics

Experimental evidence for quartets?

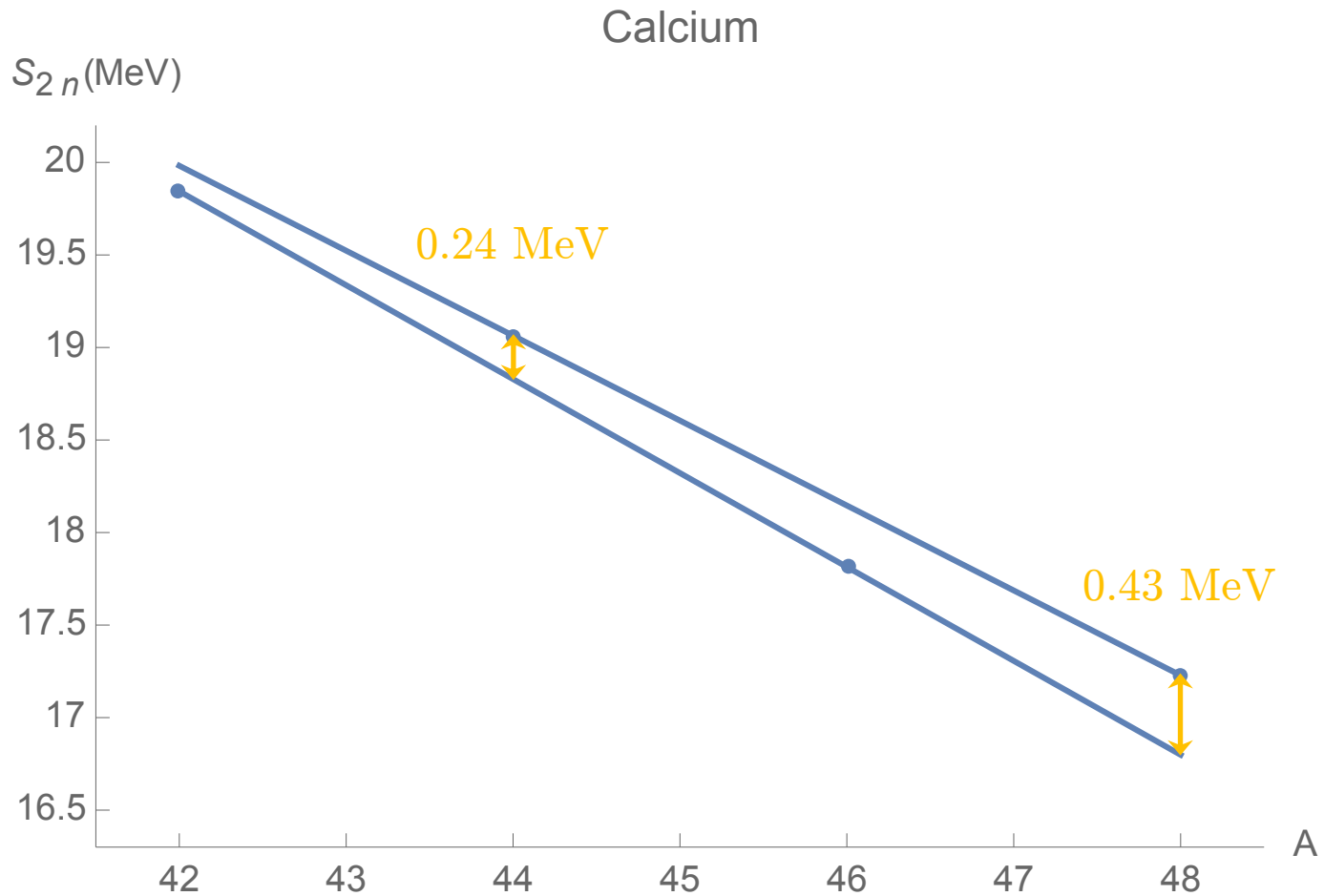


Ma, Palkanoglou, Carlson, Gandolfi, Gezerlis, D.L., Schmidt, Yu, in progress

Oxygen



Ma, Palkanoglou, Carlson, Gandolfi, Gezerlis, D.L., Schmidt, Yu, in progress



Ma, Palkanoglou, Carlson, Gandolfi, Gezerlis, D.L., Schmidt, Yu, in progress

Summary and outlook

We have presented evidence for multimodal superfluidity with simultaneous S-wave and P-wave pairing as well as quartet condensation. The phenomenon is seen in attractive extended Hubbard models in 1, 2, 3 dimensions as well as realistic neutron matter using N3LO chiral interactions. We have also presented experimental evidence in neutron-rich nuclei.

Part II: Parametric Matrix Models

Eigenvector Continuation and Parametric Matrix Models

Consider the one-parameter affine problem

$$H(c) = H_0 + cH_1$$

We now do eigenvector continuation with d training vectors. This corresponds to solving the eigenvalue problem for the new one-parameter affine system,

$$M(c) = M_0 + cM_1$$

where the matrices are d by d .

Note that the eigenvalues will be roots of the characteristic polynomial

$$P[E(c)] = \det [E(c)I - M(c)] = \det [E(c)I - M_0 - cM_1]$$

The polynomial P will be degree d in with respect to $E(c)$ and degree d with respect to c .

In contrast with polynomial interpolation or rational interpolation (Padé approximants), eigenvector continuation is performing algebraic interpolation using roots of polynomials.

Suppose that we don't have access to the training vectors. We can still make a matrix model

$$M(c) = M_0 + cM_1$$

The unknown elements of these matrices are learned using the training data for the eigenvalues $E(c)$. This is a simple example of a general technique called parametric matrix models (PMM).

Instead trying to directly fit some output functions, we try to learn the set of matrix equations whose solutions produce the output functions. This is similar to how we usually solve physics problems. We start from the equations.

Basic form for parametric matrix models

Input features

$$\{c_1, c_2, \dots, c_{N_c}\}$$

Hermitian or unitary primary matrices that are analytic functions of the input features

$$\{P_1, P_2, \dots, P_{N_P}\}$$

Normalized eigenvectors of primary matrices

$$\{v_1^{(1)}, v_1^{(2)}, \dots, v_2^{(1)}, \dots, v_{N_P}^{(1)}, \dots\}$$

Secondary matrices that are analytic functions of the input features

$$\{S_1, S_2, \dots, S_{N_P}\}$$

Scalar outputs

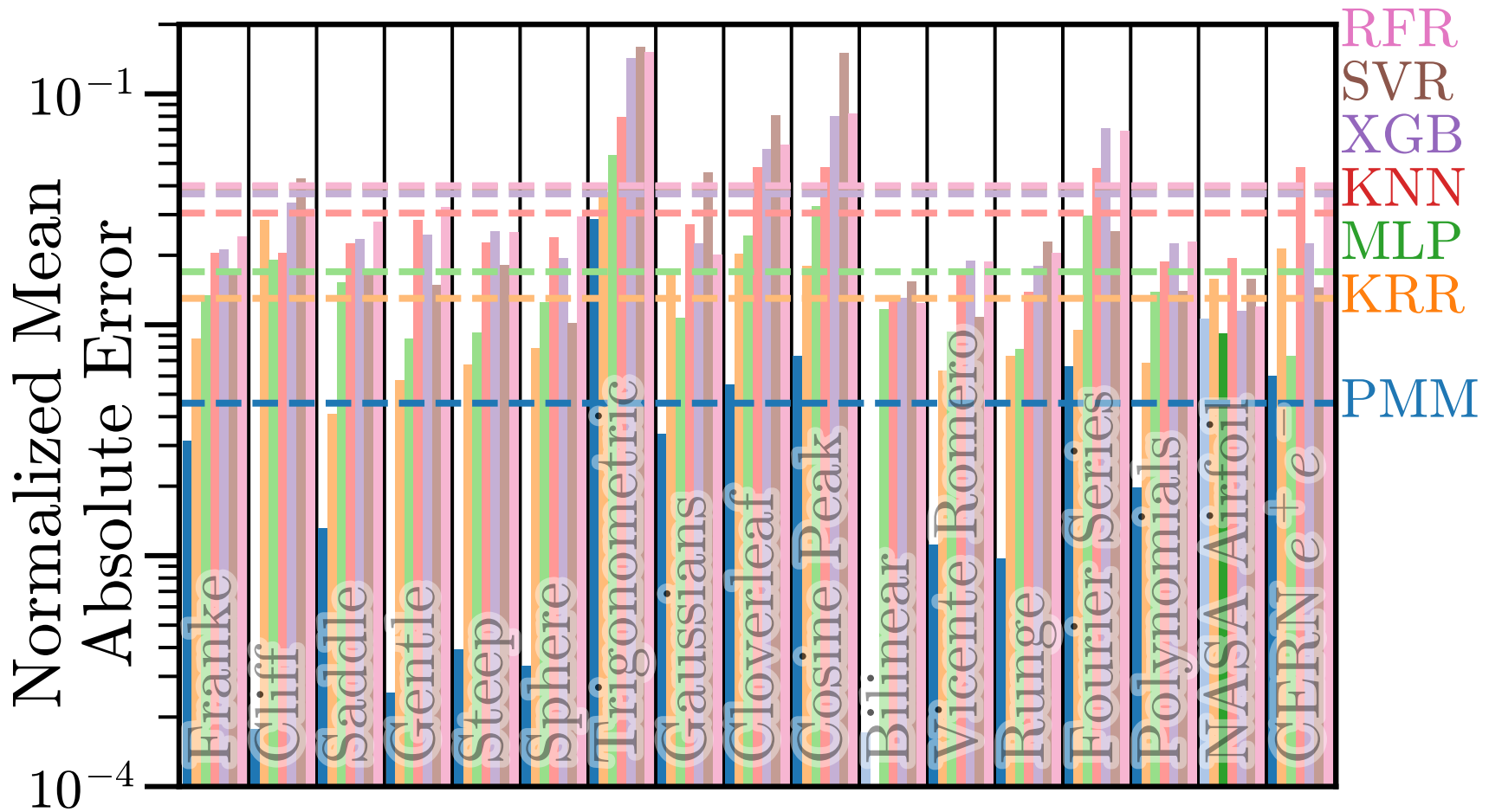
$$\{v_j^{(i)\dagger} S_k v_{j'}^{(i')}, \dots\}$$

Application to multivariate function interpolation

Name	Equation
Franke ^{†36,38}	$\frac{3}{4} \exp\left\{-\frac{(9x-2)^2+(9y-2)^2}{4}\right\} + \frac{3}{4} \exp\left\{-\frac{(9x+1)^2-9y+1}{49}\right\} + \frac{1}{2} \exp\left\{-\frac{(9x-7)^2+(9y-3)^2}{4}\right\} - \frac{1}{5} \exp\left\{-(9x-4)^2-(9y-7)^2\right\}$
Cliff ^{†38}	$\frac{1}{9} \tanh[9(y-x)] + \frac{1}{9}$
Saddle ^{†38}	$\frac{5/4 + \cos(27y/5)}{6 + 6(3x-1)^2}$
Gentle ^{†38}	$\frac{1}{3} \exp\left\{-\alpha \left[(x-\frac{1}{2})^2 + (y-\frac{1}{2})^2\right]\right\}, \quad \alpha = 81/16$
Steep ^{†38}	$\frac{1}{3} \exp\left\{-\alpha \left[(x-\frac{1}{2})^2 + (y-\frac{1}{2})^2\right]\right\}, \quad \alpha = 81/4$
Sphere ^{†38}	$-\frac{1}{2} + \sqrt{\left(\frac{8}{9}\right)^2 - \left(x-\frac{1}{2}\right)^2 - \left(y-\frac{1}{2}\right)^2}$
Trigonometric ^{†38}	$2 \cos(10x) \sin(10y) + \sin(10xy)$
Gaussians ^{†38}	$\exp\{-u^2/2\} + \frac{3}{4} \exp\{-v^2/2\} [1 + \exp\{-u^2/2\}], \quad \begin{cases} u = 5 - 10x \\ v = 5 - 10y \end{cases}$
Cloverleaf ^{†38}	$\left[\left(\frac{20}{3}\right)^3 uv\right]^2 \left[\left(\frac{1}{1+u}\right)\left(\frac{1}{1+v}\right)\right]^5 \left[u - \frac{2}{1+u}\right] \left[v - \frac{2}{1+v}\right], \quad \begin{cases} u = \exp\left\{\frac{10-20x}{3}\right\} \\ v = \exp\left\{\frac{10-20y}{3}\right\} \end{cases}$
Cosine Peak ^{†38}	$\exp\left\{-\frac{2}{3}r\right\} \cos\left(\frac{3}{2}r\right), \quad r = \sqrt{(8x-4)^2 + (9y-\frac{9}{2})^2}$
Bilinear ^{†38}	$xy + x$
Vicente Romero ^{†37,38}	$\frac{6}{5}r + \frac{21}{40} \sin\left(\frac{12\pi}{5\sqrt{2}}r\right) \sin\left[\frac{13}{10} \operatorname{atan}2(y,x)\right], \quad r = \sqrt{x^2 + y^2}$
Runge ^{†35,38}	$\left[(10x-5)^2 + (10y-5)^2 + 1\right]^{-1}$
Fourier series [‡]	$\sum_{n=1}^N \sum_{m=1}^M \left[a_{nm} \sin\left(\frac{n\pi x}{3}\right) \sin\left(\frac{m\pi y}{3}\right) + b_{nm} \cos\left(\frac{n\pi x}{3}\right) \cos\left(\frac{m\pi y}{3}\right) \right], \quad a_{nm}, b_{nm} \sim \mathcal{N}(0,1)$
Polynomials [‡]	$\sum_{n=0}^N \sum_{m=0}^M a_{nm} x^n y^m, \quad a_{nm} \sim \mathcal{N}(0,1)$

† $(x,y) \in [0,1] \times [0,1]$

‡ $(x,y) \in [-1,1] \times [-1,1]$



Parametric Matrix Model (PMM), Kernel Ridge Regression (KRR), Multilayer Perceptron (MLP), k-Nearest Neighbors (KNN), Extreme Gradient Boosting (XGB), Support Vector Regression (SVR), and Random Forest Regression (RFR)

All-order summation of perturbation theory

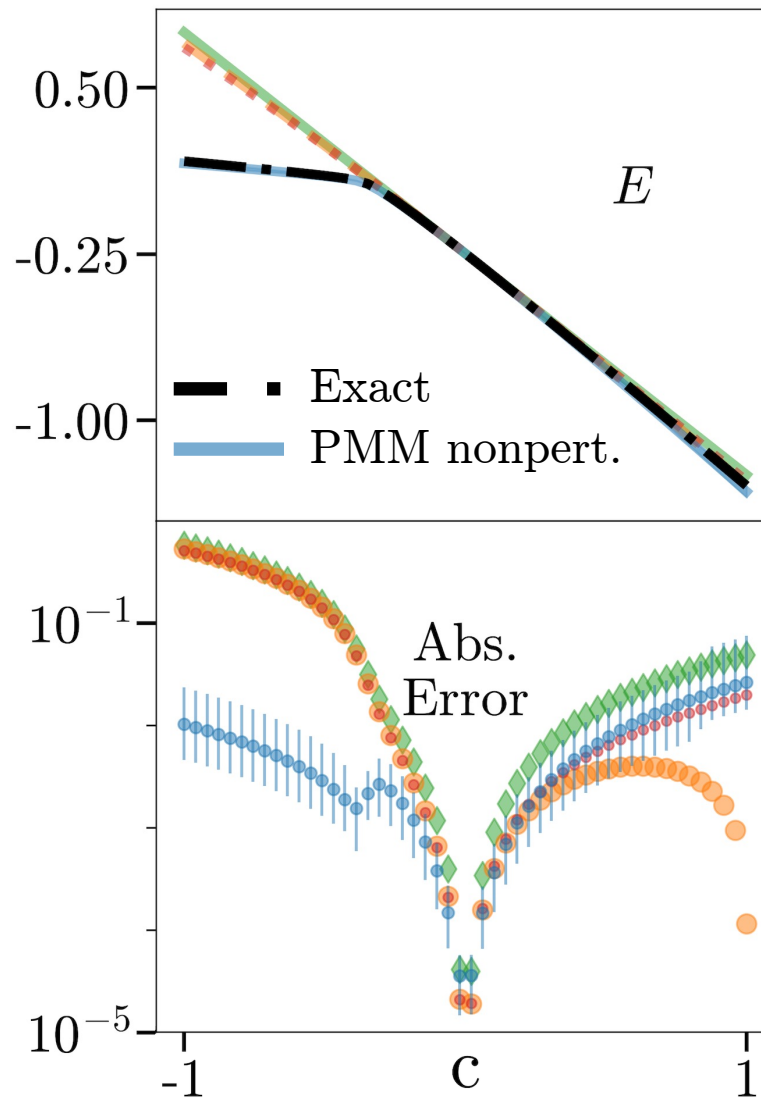
$$\boxed{} = M_{\text{LO}} =: e^{-H_{\text{LO}}d\tau} : \quad \boxed{} = O$$

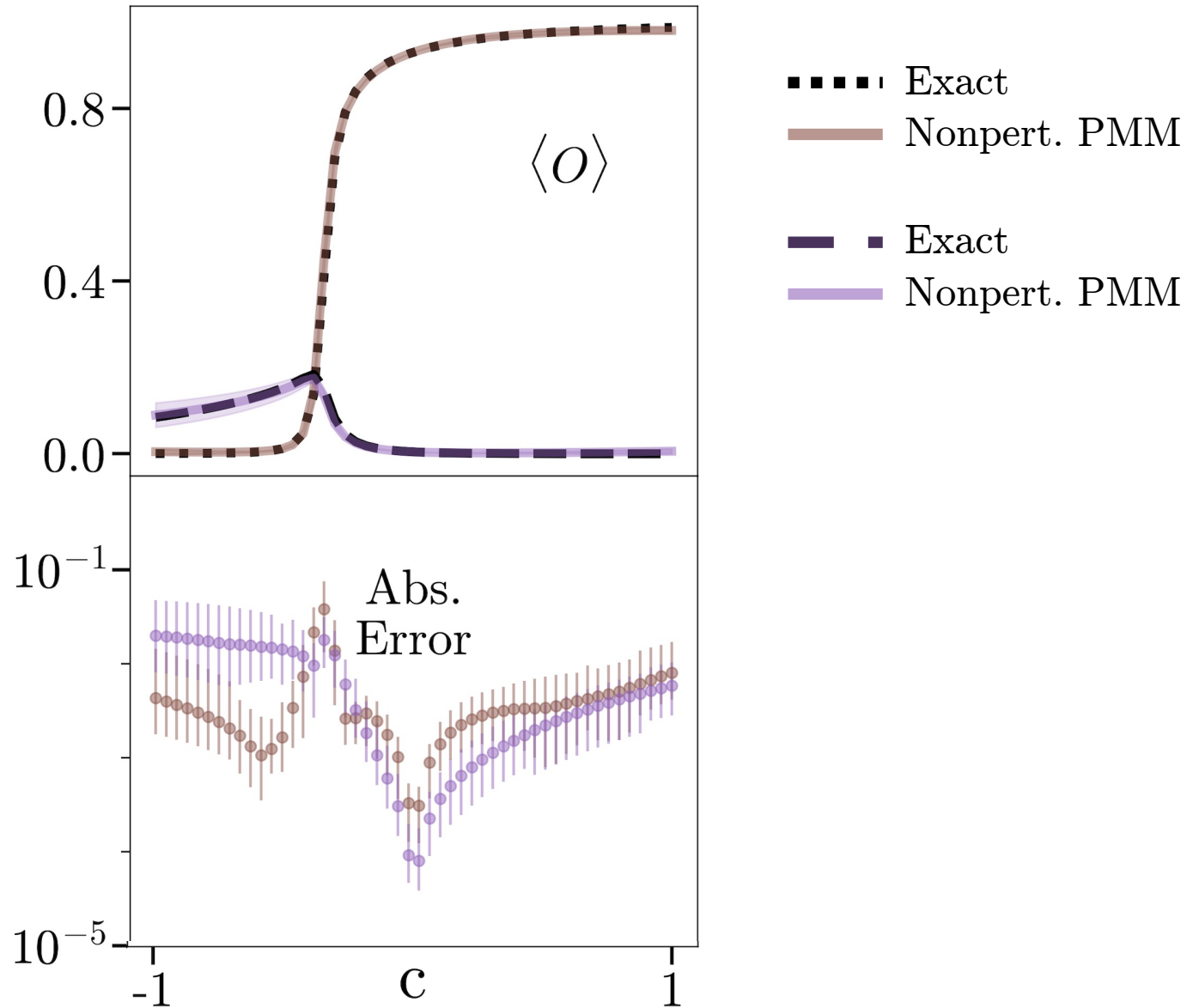
$$Z_{n_t, i, j} = \langle \psi_{\text{init}, i} | \boxed{} | \psi_{\text{init}, j} \rangle$$

$$Z_{n_t, i, j}^O = \langle \psi_{\text{init}, i} | \boxed{} \boxed{} | \psi_{\text{init}, j} \rangle$$

$$O = H_{\text{NLO}}, H_{\text{N}^2\text{LO}}, H_{\text{N}^3\text{LO}}, \dots, F[\rho(\vec{r})], \dots$$

Make a low-dimensional parametric matrix model to represent vectors and matrices in the subspace of low-energy states of H_{LO} . Then diagonalize to get nonperturbative eigenvectors. Extrapolate in the dimensions of the parametric model to eliminate systematic errors.





Summary and outlook

We briefly discussed a new machine learning approach called parameter matrix models that uses the matrix equations of physics. There appear to be numerous applications across different fields.